



Contents lists available at ScienceDirect

European Journal of Medicinal Chemistry

journal homepage: <http://www.elsevier.com/locate/ejmech>

Original article

Exploring the effects of linker composition on site-specifically modified antibody–drug conjugates

Aaron E. Albers, Albert W. Garofalo, Penelope M. Drake, Romas Kudirka, Gregory W. de Hart, Robyn M. Barfield, Jeanne Baker, Stefanie Banas, David Rabuka*

Redwood Bioscience, 5703 Hollis Street, Emeryville, CA 94608, USA

ARTICLE INFO

Article history:

Received 5 June 2014

Received in revised form

21 August 2014

Accepted 22 August 2014

Available online xxx

Keywords:

Antibody–drug conjugate

Noncleavable linker

Aldehyde tag

ABSTRACT

In the context of antibody–drug conjugates (ADCs), noncleavable linkers provide a means to deliver cytotoxic small molecules to cell targets while reducing systemic toxicity caused by nontargeted release of the free drug. Additionally, noncleavable linkers afford an opportunity to change the chemical properties of the small molecule to improve potency or diminish affinity for multidrug transporters, thereby improving efficacy. We employed the aldehyde tag coupled with the hydrazino-iso-Pictet-Spengler (HIPS) ligation to generate a panel of site-specifically conjugated ADCs that varied only in the noncleavable linker portion. The ADC panel comprised antibodies carrying a maytansine payload ligated through one of five different linkers. Both the linker-maytansine constructs alone and the resulting ADC panel were characterized in a variety of in vitro and in vivo assays measuring biophysical and functional properties. We observed that slight differences in linker design affected these parameters in disparate ways, and noted that efficacy could be improved by selecting for particular attributes. These studies serve as a starting point for the exploration of more potent noncleavable linker systems.

© 2014 Elsevier Masson SAS. All rights reserved.

1. Introduction

Antibody–drug conjugates (ADCs) promise to alter the landscape of anti-cancer therapeutics by targeting highly cytotoxic drug molecules directly to cancer cells. The success of currently approved ADCs has inspired a spate of research and development efforts in the area; dozens of new ADCs are in pre-clinical or clinical trials [1]. ADCs comprise a monoclonal antibody, a cytotoxic payload, and a linker that joins them together [2]. The monoclonal antibody targets the payload to cells expressing the antigen on their surface, and the cytotoxic payload kills the cells upon internalization of the ADC. The linker is literally the central component of an ADC; it contains the reactive group that governs the conjugation chemistry, and serves as a chemical spacer that physically connects the drug payload to the antibody. As such, the linker is also the most versatile aspect of the ADC. It can be modified in any number of ways to influence various drug/linker characteristics (e.g., solubility) [3,4] and ADC properties (e.g., potency, pharmacokinetics, therapeutic index, and efficacy in multidrug resistant cells) [5–11].

There are essentially two broad classes of ADC linkers; those that are chemically labile or enzymatically-cleavable, and those that are chemically stable or noncleavable [12]. Labile/cleavable linkers are designed to keep the ADC intact when in circulation but release the drug payload upon internalization by the target cell. Some cytotoxic payloads—for example, MMAE—require a cleavable linker, as they do not tolerate substitutions [13,14]. By contrast, other cytotoxic payloads—for example, maytansine—can accommodate substitutions while maintaining potency [15]. Such drugs are good substrates for the development of noncleavable linkers. By design, noncleavable linkers do not contain chemical functionalities that are readily susceptible to intracellular degradation. Therefore, after an internalized ADC is trafficked to the lysosome, the antibody moiety is proteolytically degraded into amino acids while the cytotoxic drug remains attached via the linker to an amino acid residue [16]. The retention of the linker as part of the active metabolite allows for the modulation of the overall properties of the metabolite (e.g., by altering hydrophobicity, length, and charge) in order to improve potency.

We previously reported a novel site-specific ligation chemistry that takes advantage of an aldehyde-tagged protein [17]. The aldehyde tag is a straightforward means of site-specifically functionalizing proteins for chemical modification. The genetically-encoded tag consists of a pentapeptide sequence (CXPXR) that is

* Corresponding author.

E-mail address: drabuka@redwoodbioscience.com (D. Rabuka).

specifically recognized by formylglycine-generating enzyme (FGE) [18–20]. During protein expression in cells, the cysteine residue in the sequence is recognized by FGE and oxidized co-translationally to formylglycine. The resulting aldehyde affords a bioorthogonal chemical handle for ligation (Fig. 1). Linkers terminating in a 2-((1,2-dimethylhydrazinyl)methyl)-1*H*-indole react with the aldehyde by way of a hydrazino-*iso*-Pictet-Spengler (HIPS) reaction to form an azacarboline, resulting in a stable C–C bond joining the antibody and payload.

The aldehyde tag platform allows for site-specific conjugation that yields a highly homogenous product. Accordingly, this technology is well-suited for performing structure activity relationship studies in the context of an intact ADC. Here, we isolated linker composition as a single variable for optimization while the other ADC components—antibody backbone, cytotoxic payload, conjugation site, drug-to-antibody ratio, and conjugation chemistry—were held constant. By characterizing a panel of five drug/linkers and their corresponding conjugates, we explored the impact of small changes in linker design on ADC potency and stability.

2. Materials and methods

2.1. Linker synthesis

Synthetic routes and analytical data are provided in the [Supplemental materials](#).

2.2. Microtubule polymerization assay

We used the Tubulin Polymerization Assay Kit (Cytoskeleton) according to the manufacturer's instructions for the fluorescence-based test. All test articles were used at 3 μ M.

2.3. Direct ELISA antigen binding

Maxisorp 96-well plates (Nunc) were coated overnight at 4 °C with 1 μ g/mL of human HER2-His (Sino Biological) in PBS. The plate was blocked with ELISA blocker blocking buffer (ThermoFisher), and then the α HER2 wild-type antibody and ADCs were plated in an 8-step series of 2-fold dilutions starting at 100 ng/mL. The plate was incubated, shaking, at room temperature for 2 h. After washing in PBS 0.1% Tween-20, bound analyte was detected with a donkey anti-human Fc- γ -specific horseradish peroxidase (HRP)-conjugated secondary antibody. Signals were visualized with Ultra TMB (Pierce) and quenched with 2 N H₂SO₄. Absorbance at 450 nm was determined using a Molecular Devices SpectraMax M5 plate reader and the data were analyzed using GraphPad Prism.

2.4. Bioconjugation, purification, and HPLC analytics

Humanized anti-HER2 IgG antibodies (15 mg/mL) bearing the aldehyde tag (LCTPSR) at the C-terminus of the heavy chain were conjugated to maytansine-containing drug linkers (8 mol equivalents drug:antibody) for 72 h at 37 °C in 50 mM sodium citrate, 50 mM NaCl pH 5.5 containing 0.85% DMA and 0.085% Triton X-100. Free drug was removed using tangential flow filtration. Unconjugated antibody was removed using preparative-scale hydrophobic interaction chromatography (HIC; GE Healthcare 17-5195-01) with mobile phase A: 1.0 M ammonium sulfate, 25 mM sodium phosphate pH 7.0, and mobile phase B: 25% isopropanol, 18.75 mM sodium phosphate pH 7.0. An isocratic gradient of 33% B was used to elute unconjugated material, followed by a linear gradient of 41–95% B to elute mono- and diconjugated species. To determine the DAR of the final product, ADCs were examined by analytical HIC (Tosoh #14947) with mobile phase A: 1.5 M ammonium sulfate, 25 mM sodium phosphate pH 7.0, and mobile phase B: 25% isopropanol, 18.75 mM sodium phosphate pH 7.0. To determine aggregation, samples were analyzed using analytical size exclusion chromatography (SEC; Tosoh #08541) with a mobile phase of 300 mM NaCl, 25 mM sodium phosphate pH 6.8.

2.5. In vitro cytotoxicity

The HER2-positive breast carcinoma cell line, NCI-N87, was obtained from ATCC and maintained in RPMI-1640 medium (Cellgro) supplemented with 10% fetal bovine serum (Invitrogen) and Glutamax (Invitrogen). 24 h prior to plating, cells were passaged to ensure log-phase growth. On the day of plating, 5000 cells/well were seeded onto 96-well plates in 90 μ L normal growth medium supplemented with 10 IU penicillin and 10 μ g/mL streptomycin (Cellgro). Cells were treated at various concentrations with 10 μ L of diluted analytes, and the plates were incubated at 37 °C in an atmosphere of 5% CO₂. After 6 d, 100 μ L/well of CellTiter-Glo reagent (Promega) was added, and luminescence was measured using a Molecular Devices SpectraMax M5 plate reader. GraphPad Prism software was used for data analysis, including IC₅₀ calculations.

2.6. In vitro stability

ADCs were spiked into rat plasma at ~1 pmol (payload)/mL. The samples were aliquoted and stored at –80 °C until use. Aliquots were placed at 37 °C under 5% CO₂ for the indicated times and then were analyzed by ELISA to assess the anti-maytansine and anti-Fab signals. A freshly thawed aliquot was used as a reference starting value for conjugation. All analytes were measured together on one plate to enable comparisons across time points. First, analytes were

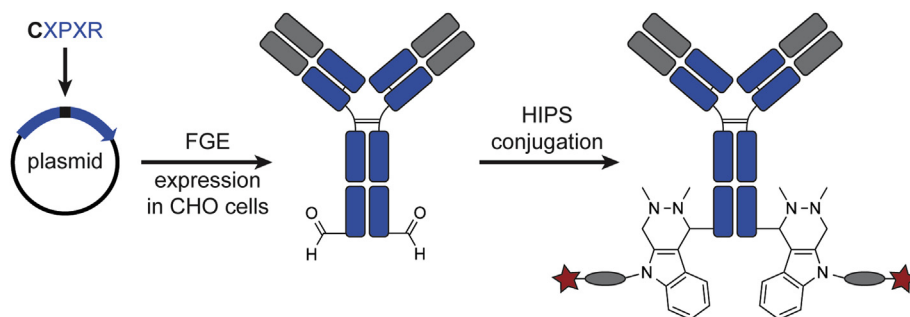


Fig. 1. The aldehyde tag coupled with HIPS ligation yields site-specifically modified antibodies. Using standard molecular biology techniques, a formylglycine-generating enzyme (FGE) recognition sequence (CXPXR) is site-specifically inserted into the backbone of the antibody. FGE co-translationally oxidizes the cysteine residue to formylglycine. The aldehyde of formylglycine can then be reacted with nucleophiles to form a stable C–C bond.

diluted in blocking buffer to 20 ng/mL (within the linear range of the assay). Then, analytes were captured on plates coated with an anti-human Fab-specific antibody. Next, the payload was detected with an anti-maytansine antibody followed by an HRP-conjugated secondary; the total antibody was detected with a directly conjugated anti-human Fc-specific antibody. Bound secondary antibody was visualized with TMB substrate. The colorimetric reaction was stopped with H₂SO₄, and the absorbance at 450 nm was determined using a Molecular Devices SpectraMax M5 plate reader. Data analysis was performed in Excel. Each sample was analyzed in quadruplicate, and the average values were used. The ratio of anti-maytansine signal to anti-Fab signal was used as a measure of antibody conjugation.

2.7. Xenograft studies

The animal studies were approved by Charles River Laboratories Institutional Animal Care and Use Committee (IACUC). Female C.B-17 SCID mice were inoculated subcutaneously with 1×10^7 NCI-N87 tumor cells in 50% Matrigel. When the tumors reached an average of 112 mm³, the animals were given a single 5 mg/kg dose of ADC, trastuzumab antibody (untagged), or vehicle alone. The animals were monitored twice weekly for body weight and tumor size. Tumor volume was calculated using the formula:

$$\text{Tumor volume (mm}^3\text{)} = \frac{w^2 \times l}{2}$$

where w = tumor width and l = tumor length.

Tumor doubling times were obtained by averaging the tumor growth rate curves from four groups of mice. Then, log₁₀ cell kill was estimated using the formula:

$$\log_{10} \text{ cell kill} = \frac{\text{treated group TTE} - \text{control group TTE}}{3.32 \times \text{tumor doubling time}}$$

Treatment over control (T/C) ratios were determined by dividing the tumor volume of the treatment group by the tumor volume of the control group at a designated time point.

3. Results and discussion

3.1. Linker design and synthesis

To examine the effect of linker composition, we tested a variety of maytansine-linkers that contained functional groups anticipated to aid in solubility, which improves bioconjugation yields [4]. Initially, we used PEG_{*n*} spacers (with $n = 2, 4, \text{ or } 6$), but found that the PEG group alone was not sufficiently hydrophilic to overcome the very hydrophobic contributions from the maytansine and HIPS components. The conjugation efficiencies observed with linkers containing PEG_{*n*} spacers alone were poor, e.g., 40% yield with a PEG₆-maytansine linker conjugated to a C-terminally-tagged antibody. We found that a simple way to incorporate hydrophilicity was by using amino acid residues as linker components (Fig. 2). In turn, this change resulted in a significant improvement in conjugation efficiency, e.g., 90% yield with a glutamic acid PEG₂-maytansine linker conjugated to a C-terminally-tagged antibody. Here, we tested the effect of using different amino acids as solubilizing agents by evaluating glutamic acid (Linkers 1, 4, and 5), asparagine (Linker 2), and phosphotyrosine (Linker 3). The latter was meant to function as a pro-drug, where the phosphorylated form would be soluble, but not membrane permeable. Once inside a cell, the linker was intended to be a substrate for phosphorylases, the action of which would yield a more hydrophobic and membrane-permeable

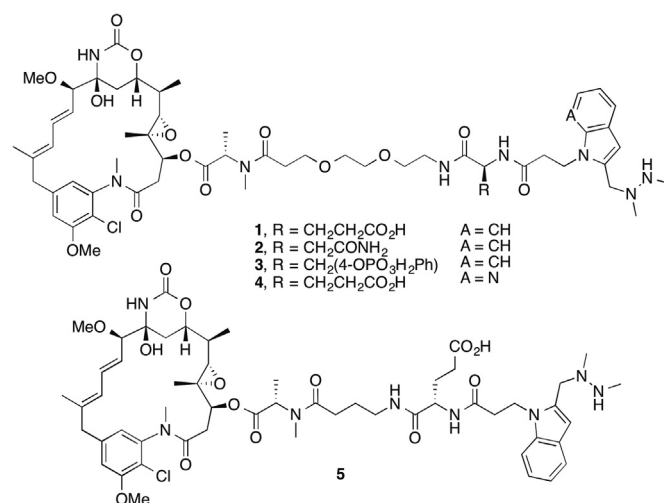


Fig. 2. Inclusion of amino acid residues resulted in highly soluble maytansine-linker constructs with varied chemical composition. Five different maytansine-conjugated linkers were synthesized (as shown in Scheme 1) and characterized, both as free drugs and after conjugation to an α -HER2 antibody.

active metabolite. We also incorporated a spacer element into the linkers—either PEG₂ or *n*-propyl—to improve conjugation efficiency and mitigate ADC aggregation. Finally, taking advantage of the hydrazino-*iso*-Pictet-Spengler (HIPS) chemistry, the linkers terminated in either a reactive 2-((1,2-dimethylhydrazinyl)methyl)indole (1, 2, 3, and 5) or 2-((1,2-dimethylhydrazinyl)methyl)pyrrolo [2,3-*b*]pyridine (4). The latter varied from the former by a single nitrogen atom (Fig. 2), making it slightly more hydrophilic. Both reactive groups enabled HIPS ligation of the linker-maytansine to aldehyde-tagged antibodies for ADC production.

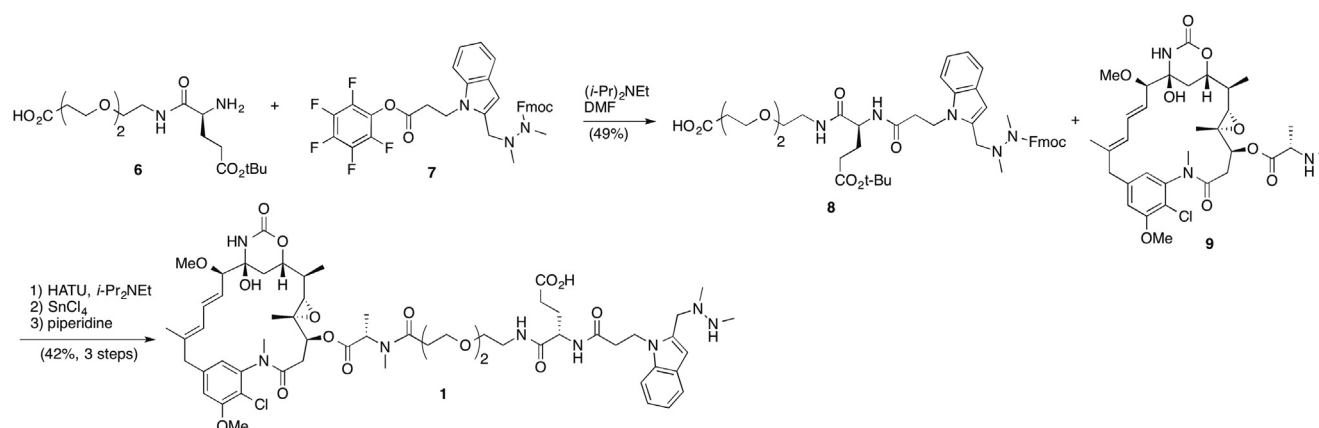
A representative synthesis of the linkers is shown in Scheme 1. In the example, a pegylated, protected amino acid, 6, is coupled to pentafluorophenyl ester, 7. The product, 8, is then coupled to *N*-deacetylmaytansine, 9, using HATU followed by hydrolysis of the *tert*-butyl ester and removal of the Fmoc-protecting group with piperidine to give the final desired product, 1.

3.2. Linker composition did not alter the payload's ability to inhibit microtubule polymerization

As a first step, once the drug/linkers were in hand, we performed an *in vitro* microtubule polymerization assay to confirm that the incorporated structural variations and elaborations to maytansine did not impair the drug's ability to inhibit microtubule polymerization (Fig. 3). As anticipated, due to the known tolerance of maytansine to substitutions at the *N*-acyl position [21], the panel of drug/linkers resulted in microtubule polymerization inhibition similar to unmodified maytansine. A small spread of values was noted, but all were within 32% of maytansine itself. As shown in the next section, these small differences did not appear to impact the IC₅₀ of the drug/linkers when formulated as an ADC.

3.3. Bioconjugation and *in vitro* assessment of the ADC panel

Conjugation of the drug/linkers to a C-terminally aldehyde tagged α -HER2 antibody was carried out by treating the antibody at 37 °C with 8–10 equivalents of linker-maytansine in 50 mM sodium citrate, 50 mM NaCl pH 5.5 containing 0.85% DMA and 0.085% Triton X-100, and the progress of the reaction was tracked by analytical hydrophobic interaction chromatography (HIC). Upon completion, the excess payload was removed by tangential flow



Scheme 1. Representative linker synthesis.

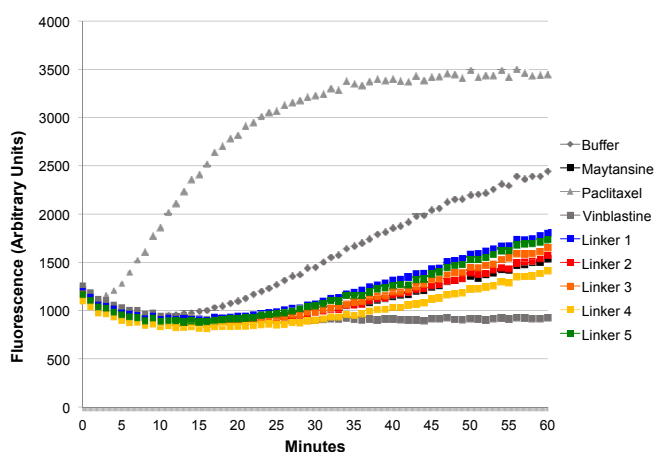


Fig. 3. Linker selection does not hinder maytansine inhibition of microtubule polymerization. The drug/linkers were tested in a microtubule polymerization assay. Free maytansine was included as a positive control. Paclitaxel and vinblastine were included as a promoter and inhibitor, respectively, of microtubule polymerization. The buffer control indicates the polymerization rate of untreated microtubules. Relative to free maytansine, the drug/linkers inhibited polymerization by the following amounts: Linker 1, 68%; Linker 2, 92%; Linker 3, 79%; Linker 4, 105%; Linker 5, 73%.

filtration, and the unconjugated antibody was removed by preparative HIC. These reactions were high yielding, with >90% conjugation efficiency (Table S1). After purification, the ADCs contained an average drug-to-antibody ratio (DAR) of 1.6 as determined by hydrophobic interaction chromatography (Figure S2). The drug distribution (ratio of DAR 1–2) was very similar among the ADCs made with different linkers (Table S2). The preparations were $\geq 95\%$ monomeric as assessed by size-exclusion chromatography (data not shown).

With the ADCs in hand, we first asked whether conjugation with the drug/linkers had altered the antibody affinity for the HER2 antigen. To test this, we performed a direct-binding ELISA assay using plates coated with human HER2-His, and compared the EC_{50} of the wild-type (untagged and unconjugated) α -HER2 to the values obtained for the panel of α -HER2 ADCs (Fig. 4). Only minimal differences in affinity were noted, with most of the ADCs appearing to bind with slightly higher affinity than the wild-type antibody.

Next, we tested the *in vitro* cytotoxicity of the ADCs against the HER2-overexpressing gastric cell line, NCI-N87 (Fig. 5A). As a comparator, we also tested the cytotoxic activity of the corresponding free drug/linkers (Fig. 5B). Cell cultures were exposed to

varying concentrations of the analytes for 6 days, and then cell viability was measured by using a CellTiter-Glo assay, which quantifies ATP levels. All ADCs exhibited picomolar activity, with IC_{50} values similar to or better than that observed after treatment with free maytansine. By contrast to the ADCs, the free drug/linkers were overall less potent, generally showing IC_{50} values that were 1000- to 2000-fold higher than the corresponding ADCs. Linkers 1 and 4, which shared a glutamic acid-PEG₂ scaffold, both had free drug/linker IC_{50} values above 1 μ M, $\sim 10,000$ -fold higher than the ADC versions of those compounds. In addition to the IC_{50} values, we noted that the Linker 3 ADC, in spite of its measured picomolar activity, failed to kill more than 70% of the cells, even at the highest doses (Fig. 5A). The free version of Linker 3 did not suffer from this same cytotoxic plateau, reducing cell viability by >93% at the highest dose (Fig. 5B). We observed the same trends with the unconjugated and conjugated versions of Linker 3 on a different antibody and against a different cell line, suggesting that the plateau effect of this linker is translatable across platforms. Although the cytotoxic plateau is commonly observed in these types of assays, the underlying mechanisms involved and the biological significance of the effect is not clear.

As a final *in vitro* characterization of the ADC panel, we examined the stability of the HIPS-conjugates in plasma for 14 days at 37 °C. The assay consisted of an ELISA-based method that compared the ratio of anti-payload to anti-Fc signals. As a group, the conjugates exhibited a high degree of stability, with $\geq 85\%$ payload remaining after 7 days and $\geq 74\%$ payload remaining after 14 days (Table 1). The glutamic acid-PEG₂-containing scaffolds were the most stable over 14 days, both demonstrating more than 80% retention of payload. The most labile linker, Linker 2, only differed from the most stable linker by about 10% over 14 days.

3.4. *In vivo* efficacy of the ADC panel

To test the *in vivo* efficacy of the ADC panel, we assessed the conjugates using an NCI-N87 xenograft model in SCID mice. Compounds were administered as a single 5 mg/kg dose at the onset of the study. All ADCs were well-tolerated with no animal showing >10% weight loss up to 40 days post-treatment (Figure S1). Tumor growth was arrested, and some tumors were reduced in size after treatment with the α -HER2 ADCs (Fig. 6A), but not after treatment with the isotype control ADC (conjugated using Linker 1). Eventually, tumors began to regrow in all animals, sooner in some groups than others, depending on the ADC used for treatment. By 60–70 days post-dose, there were clear differences in mean tumor volumes among groups treated with an α -HER2 ADC; specifically, the

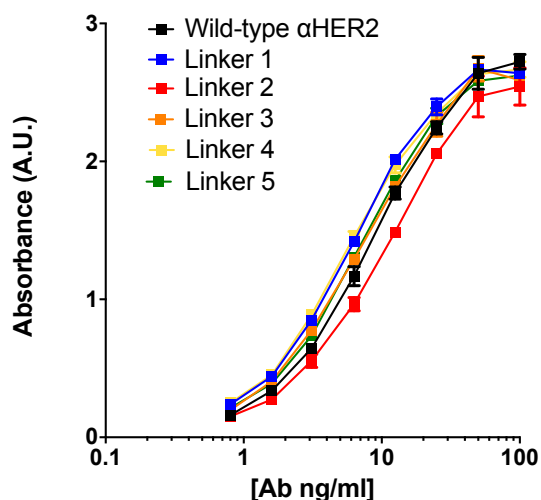


Fig. 4. α -HER2 ADCs conjugated with the panel of drug/linkers maintain their affinity for HER2 antigen. A direct-binding ELISA assay, using immobilized human HER2-His protein as the capture reagent and an anti-human Fc- γ -specific HRP-conjugated antibody as the detection reagent, was used to monitor the affinity of α -HER2 conjugates relative to the wild-type antibody. Standard curves of each analyte were generated and the EC_{50} value of each curve was calculated using GraphPad Prism. The calculated EC_{50} values (nM) were: Wild-type antibody, 8.72; Linker 1, 6.20; Linker 2, 10.80; Linker 3, 7.10; Linker 4, 5.95; Linker 5, 7.23.

mean tumor volumes ranged from 249 to 487 mm³ at day 60 (Fig. 6A). In order to investigate this effect, we looked at the log₁₀ cell kill for tumors dosed with the various treatments (Table 2). The results indicated that treatment with ADCs conjugated to Linkers 1 and 4 killed more tumor cells as compared to treatment with the other ADCs. Notably, these two linkers represented the absolute minimum amount of chemical diversity, both contained the glutamic acid-PEG₂ scaffold and differed from each other by only a single nitrogen group in the azacarboline that forms during ligation. This increased potency translated into a survival advantage for animals treated with ADCs conjugated to Linkers 1 or 4 (Fig. 6B).

The efficacy of Linker 5 was reduced as compared to Linkers 1 and 4, with which it shared the glutamic acid moiety. The results of this series of linkers suggest that, in this context, inclusion of the *n*-propyl spacer reduced efficacy as compared to the PEG₂ spacer. The other two linkers, which incorporated different amino acids on the PEG₂ scaffold, had varying efficacy. Linker 2 showed an intermediate log₁₀ cell kill value (reflecting total cells killed throughout the course of the study), but was the best performer in the first 10 days

Table 1

ADCs made with different linkers show similar stability in plasma at 37 °C.

ADC	% Conjugate remaining after 7 days	% Conjugate remaining after 14 days
α HER2-Linker 1	93	81
α HER2-Linker 2	85	74
α HER2-Linker 3	93	77
α HER2-Linker 4	97	83
α HER2-Linker 5	95	77

of the study, reducing tumor volume more than any other treatment (Fig. 6A). Linker 3 had the poorest *in vivo* efficacy ($p < 0.007$, by the log-rank, Mantel–Cox, test). It is interesting to consider whether the incomplete *in vitro* killing of NCI-N87 target cells by ADCs conjugated to this linker is related to—or perhaps predictive of—its reduced *in vivo* efficacy as compared to the other ADCs.

Next, we selected two linkers from the initial panel to take into a multidose efficacy study. We chose Linker 1 on the merits of its overall potency, as measured by tumor growth, log₁₀ cell kill, and survival. We chose Linker 2 because it showed the fastest initial tumor reduction, and we reasoned that perhaps this quick response would translate into increased efficacy in a multidose setting. The multidose study employed NCI-N87 tumors in SCID mice. Animals were dosed (10 mg/kg) once a week for four weeks. The experiment employed two arms—with dosing beginning when tumors reached average volumes of either 180 or 400 mm³. α -HER2 ADCs made with both Linkers 1 and 2 were highly active against the smaller tumors (Fig. 7A), and resulted in very similar levels of tumor control. By contrast, against the larger tumors, the α -HER2 ADC made with Linker 2 showed superior efficacy, resulting in a greater level of tumor inhibition as compared to the ADC made with Linker 1 (Fig. 7B). Specifically, the treated/control tumor volumes at day 42 were 0.39 and 0.26 for Linkers 1 and 2, respectively.

In conclusion, we developed a panel of C-terminally-conjugated α -HER2 ADCs bearing highly similar linkers, and observed that relatively minor structural changes led to dramatic differences in potency both *in vitro* and *in vivo* against the NCI-N87 tumor model. Other biophysical parameters were less impacted. Specifically, we observed only minor effects of linker architecture on inhibition of microtubule polymerization (at the free drug/linker level), and antibody affinity (at the ADC level). With respect to *in vitro* cytotoxicity, as a group, the ADCs were highly efficacious and yielded very similar IC₅₀ values, with less than a 2-fold difference

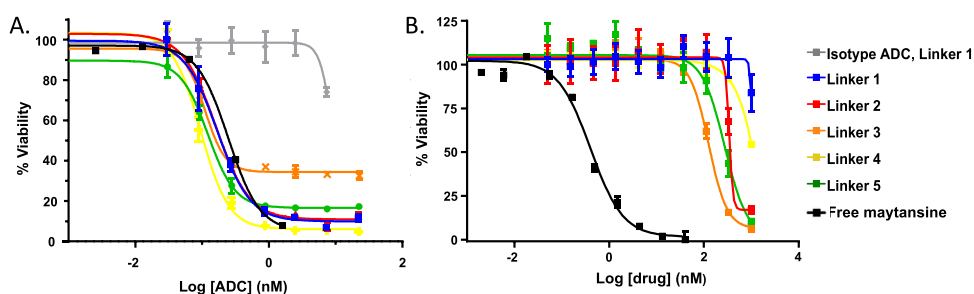


Fig. 5. Small changes in linker composition do not influence the *in vitro* cytotoxicity of α HER2 ADCs. NCI-N87 cells, which overexpress HER2, were used as targets for *in vitro* cytotoxicity in a 6 day assay. Free maytansine (black line) was included as a positive control, and an isotype control ADC (gray line) conjugated to Linker 1 was used as a negative control to indicate specificity. (A) ADC IC₅₀ values (reflecting the antibody concentrations except in the case of the free drug) were measured as follows: free maytansine, 250 pM; Linker 1, 170 pM; Linker 2, 160 pM; Linker 3, 110 pM; Linker 4, 96 pM; Linker 5, 120 pM; isotype control ADC, could not be determined. (B) Free drug/linker IC₅₀ values were measured as follows: free maytansine, 405 pM; Linker 1, 1.58 μ M; Linker 2, 342.5 nM; Linker 3, 125.8 nM; Linker 4, ~1 μ M; Linker 5, 274.9 nM.

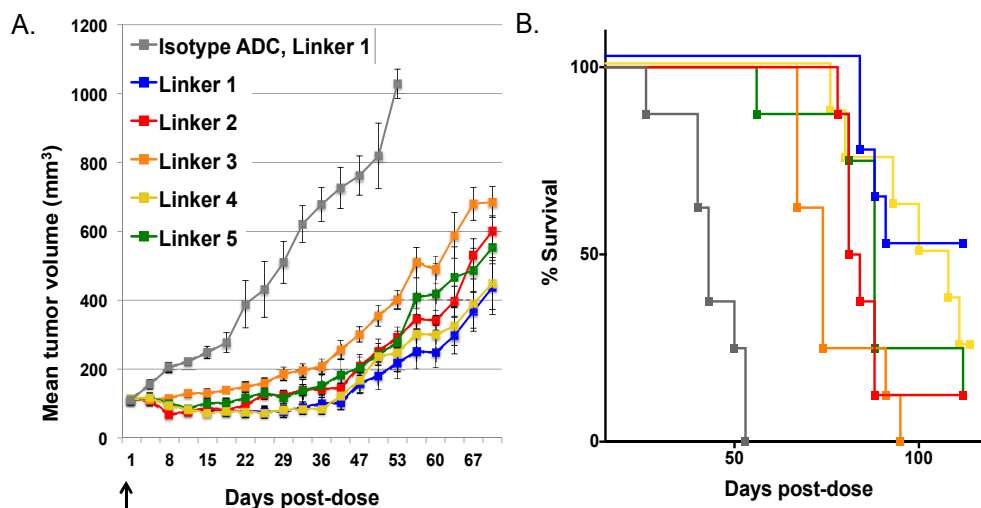


Fig. 6. Linker composition affects the in vivo efficacy of aldehyde-tagged α -HER2 ADCs in an NCI-N87 tumor model. CB.17 SCID mice (8/group) were implanted subcutaneously with NCI-N87 cells. When the tumors reached ~ 113 mm³, the animals were given a single 5 mg/kg dose of an α -HER2 conjugated to Linkers 1–5 or of an isotype control antibody conjugated to Linker 1. (A) Tumor growth was monitored twice weekly. (B) The differences in efficacy among the ADCs tested were reflected in survival curves. Animals were euthanized when tumors reached 800 mm³ or on day 112 of the study, whichever occurred first.

Table 2

In vivo log₁₀ cell kill of NCI-N87 tumor cells achieved by a single 5 mg/kg ADC dose.

α -HER2 ADC linker composition	Log ₁₀ cell kill
Linker 1	1.24
Linker 2	0.82
Linker 3	0.65
Linker 4	1.22
Linker 5	0.92

encompassing the entire panel. However, one ADC—conjugated with Linker 3—exhibited a striking viability plateau in vitro, with 32% viable cells remaining at the highest doses. By contrast to the ADCs, the potency of the free drug/linkers varied more widely, with a 12-fold difference encompassing the range of IC₅₀ values. Interestingly, the rank order potency of the ADC did not directly correlate with that of the free drug/linker. Furthermore, the

“completeness” of the cell cytotoxicity was not always the same between the corresponding ADC and free drug/linker analytes. For example, treatment with free Linker 3 abrogated all but 7% of the viable cells. With respect to in vivo cytotoxicity, ADCs made with all of the linkers inhibited growth of the HER2-overexpressing NCI-N87 xenograft to some extent. However, the log₁₀ cell kill values achieved by the ADCs varied by up to 2-fold, and the median survival time among the groups differed by 17 days, indicating that linker structure affected efficacy. Furthermore, we observed a difference in the kinetics of tumor response to ADCs made with distinct linkers, e.g., Linker 2 vs. Linker 1, whereby Linker 2 was more efficacious in the short term (1 wk), but the response was short lived. We were able to capitalize on this difference in a follow up multidose xenograft study, in which the ADC with faster cytotoxic kinetics showed superior efficacy against larger tumors. Therefore, we demonstrated that the sensitivity of our system to linker design affords an opportunity to engineer next-generation ADCs with optimized characteristics for improved efficacy.

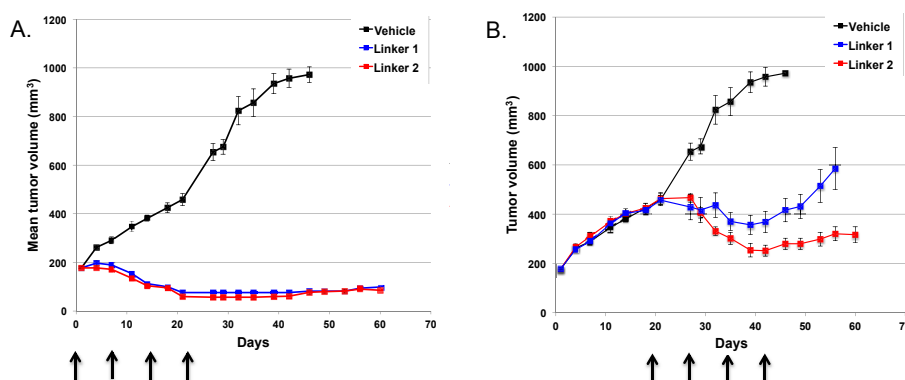


Fig. 7. Multidose xenograft studies reveal differences in efficacy against larger tumors between ADCs made with Linkers 1 and 2. CB.17 SCID mice (8/group) were implanted subcutaneously with NCI-N87 cells. Tumors were allowed to grow to either ~ 180 or 400 mm³ (Panels A and B, respectively) and then treatment was initiated. Animals were dosed once a week for four weeks with 10 mg/kg of an α -HER2 ADC conjugated to Linkers 1 or 2. Arrows indicate dosing days. Tumor growth was monitored twice weekly. Animals were euthanized when tumors reached 800 mm³.

Appendix A. Supplementary data

Supplementary data related to this article can be found at <http://dx.doi.org/10.1016/j.ejmech.2014.08.062>.

References

- [1] J.A. Flygare, T.H. Pillow, P. Aristoff, Antibody–drug conjugates for the treatment of cancer, *Chem. Biol. Drug. Des.* 81 (2012) 113–121.
- [2] R.V.J. Chari, M.L. Miller, W.C. Widdison, Antibody–drug conjugates: an emerging concept in cancer therapy, *Angew. Chem. Int. Ed. Engl.* 53 (2014) 3796–3827.
- [3] R.Y. Zhao, H.K. Erickson, B.A. Leece, E.E. Reid, V.S. Goldmacher, J.M. Lambert, R.V.J. Chari, Synthesis and biological evaluation of antibody conjugates of phosphate prodrugs of cytotoxic DNA alkylators for the targeted treatment of cancer, *J. Med. Chem.* 55 (2012) 766–782.
- [4] R.Y. Zhao, S.D. Wilhelm, C. Audette, G. Jones, B.A. Leece, A.C. Lazar, V.S. Goldmacher, R. Singh, Y. Kovtun, W.C. Widdison, J.M. Lambert, R.V.J. Chari, Synthesis and evaluation of hydrophilic linkers for antibody–maytansinoid conjugates, *J. Med. Chem.* 54 (2011) 3606–3623.
- [5] H.K. Erickson, G.D. Lewis Phillips, D.D. Leipold, C.A. Provenzano, E. Mai, H.A. Johnson, B. Gunter, C.A. Audette, M. Gupta, J. Pinkas, J. Tibbitts, The effect of different linkers on target cell catabolism and pharmacokinetics/pharmacodynamics of trastuzumab maytansinoid conjugates, *Mol. Cancer Ther.* 11 (2012) 1133–1142.
- [6] S.C. Jeffrey, J.B. Andreyka, S.X. Bernhardt, K.M. Kissler, T. Kline, J.S. Lenox, R.F. Moser, M.T. Nguyen, N.M. Okeley, I.J. Stone, X. Zhang, P.D. Senter, Development and properties of β -glucuronide linkers for monoclonal antibody–drug conjugates, *Bioconjug. Chem.* 17 (2006) 831–840.
- [7] G.D. Lewis Phillips, G. Li, D.L. Dugger, L.M. Crocker, K.L. Parsons, E. Mai, W.A. Blattler, J.M. Lambert, R.V.J. Chari, R.J. Lutz, W.L.T. Wong, F.S. Jacobson, H. Koeppen, R.H. Schwall, S.R. Kenkare-Mitra, S.D. Spencer, M.X. Sliwkowski, Targeting HER2-positive breast cancer with trastuzumab-DM1, an antibody–cytotoxic drug conjugate, *Cancer Res.* 68 (2008) 9280–9290.
- [8] S.O. Doronina, T.D. Bovee, D.W. Meyer, J.B. Miyamoto, M.E. Anderson, C.A. Morris-Tilden, P.D. Senter, Novel peptide linkers for highly potent antibody–auristatin conjugate, *Bioconjug. Chem.* 19 (2008) 1960–1963.
- [9] S.O. Doronina, B.A. Mendelsohn, T.D. Bovee, C.G. Cervený, S.C. Alley, D.L. Meyer, E. Oflazoglu, B.E. Toki, R.J. Sanderson, R.F. Zabinski, A.F. Wahl, P.D. Senter, Enhanced activity of monomethylauristatin F through monoclonal antibody delivery: effects of linker technology on efficacy and toxicity, *Bioconjug. Chem.* 17 (2006) 114–124.
- [10] S.C. Alley, D.R. Benjamin, S.C. Jeffrey, N.M. Okeley, D.L. Meyer, R.J. Sanderson, P.D. Senter, Contribution of linker stability to the activities of anticancer immunoconjugates, *Bioconjug. Chem.* 19 (2008) 759–765.
- [11] P. Strop, S.-H. Liu, M. Dorywalska, K. Delaria, R.G. Dushin, T.-T. Tran, W.-H. Ho, S. Farias, M.G. Casas, Y. Abdiche, D. Zhou, R. Chanrasekaran, C. Samain, C. Loo, A. Rossi, M. Rickert, S. Krimm, T. Wong, S.M. Chin, J. Yu, J. Dilley, J. Chaparro-Riggers, G.F. Filzen, C.J. O'Donnell, F. Wang, J.S. Myers, J. Pons, D.L. Shelton, A. Rajpal, Location matters: site of conjugation modulates stability and pharmacokinetics of antibody drug conjugates, *Chem. Biol.* 20 (2013) 161–167.
- [12] P.M. Drake, D. Rabuka, in: B. Bonavida (Ed.), *Resistance to Targeted Anti-Cancer Therapeutics*, Springer New York, New York, NY, 2013, pp. 183–200.
- [13] P.R. Hamann, R.G. Dushin, *Antibody–Drug Conjugates in Oncology* (Chapter 7), in: *New Frontiers in Chemical Biology: Enabling Drug Discovery*, The Royal Society of Chemistry, 2011, pp. 224–257. JF – JO – VL – IS –.
- [14] S.O. Doronina, B.E. Toki, M.Y. Torgov, B.A. Mendelsohn, C.G. Cervený, D.F. Chace, R.L. DeBlanc, R.P. Gearing, T.D. Bovee, C.B. Siegall, J.A. Francisco, A.F. Wahl, D.L. Meyer, P.D. Senter, Development of potent monoclonal antibody auristatin conjugates for cancer therapy, *Nat. Biotechnol.* 21 (2003) 778–784.
- [15] B.A. Kellogg, L. Garrett, Y. Kovtun, K.C. Lai, B. Leece, M. Miller, G. Payne, R. Steeves, K.R. Whiteman, W. Widdison, H. Xie, R. Singh, R.V.J. Chari, J.M. Lambert, R.J. Lutz, Disulfide-linked antibody–maytansinoid conjugates: optimization of in vivo activity by varying the steric hindrance at carbon atoms adjacent to the disulfide linkage, *Bioconjug. Chem.* 22 (2011) 717–727.
- [16] X. Sun, W. Widdison, M. Mayo, S. Wilhelm, B. Leece, R. Chari, R. Singh, H. Erickson, Design of antibody–maytansinoid conjugates allows for efficient detoxification via liver metabolism, *Bioconjug. Chem.* 22 (2011) 728–735.
- [17] P. Agarwal, R. Kudirka, A.E. Albers, R.M. Barfield, G.W. de Hart, P.M. Drake, L.C. Jones, D. Rabuka, Hydrazino-pictet–spengler ligation as a biocompatible method for the generation of stable protein conjugates, *Bioconjug. Chem.* 24 (2013) 846–851.
- [18] I.S. Carrico, B.L. Carlson, C.R. Bertozzi, Introducing genetically encoded aldehydes into proteins, *Nat. Chem. Biol. Nat. Publ. Group* 3 (2007) 321–322.
- [19] P. Wu, W. Shui, B.L. Carlson, N. Hu, D. Rabuka, J. Lee, C.R. Bertozzi, Site-specific chemical modification of recombinant proteins produced in mammalian cells by using the genetically encoded aldehyde tag, *Proc. Natl. Acad. Sci. U. S. A.* 106 (2009) 3000–3005.
- [20] D. Rabuka, J.S. Rush, G.W. deHart, P. Wu, C.R. Bertozzi, Site-specific chemical protein conjugation using genetically encoded aldehyde tags, *Nat. Protoc.* 7 (2012) 1052–1067.
- [21] Y.V. Kovtun, C.A. Audette, M.F. Mayo, G.E. Jones, H. Doherty, E.K. Maloney, H.K. Erickson, X. Sun, S. Wilhelm, O. Ab, K.C. Lai, W.C. Widdison, B. Kellogg, H. Johnson, J. Pinkas, R.J. Lutz, R. Singh, V.S. Goldmacher, R.V.J. Chari, Antibody–maytansinoid conjugates designed to bypass multidrug resistance, *Cancer Res.* 70 (2010) 2528–2537.